Article

How Do Ionic Liquids Affect the Surface Structure of Titania Photocatalyst? An Electron-Trap Distribution-Analysis Study

Justyna Łuczak, Anna Pancielejko, Guangyi Chen, Mai Takashima, Adriana Zaleska-Medynska,* and Bunsho Ohtani*

Read Online

ACCESS | Metrics & More | Article Recommendations

ABSTRACT: Titanium(IV) oxide, titania, photocatalyst particles were prepared from titanium alkoxide in the presence of several kinds of ionic liquids, and it was clarified that a group of samples exhibited photocatalytic activity for phenol degradation under the irradiation of light of wavelength >400 nm higher than those of the other group of samples. Although the conventional structural analytical results could not be related to the activity, electron-trap distribution measured by reversed double-beam photoacoustic spectroscopy suggested that a part of the ionic liquid induced the creation of a surface amorphous layer covered with hydrophobic organic residues to enhance the adsorption of phenol on the surface.
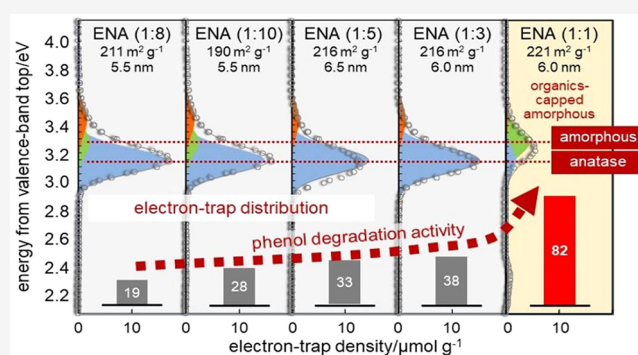
INTRODUCTION

Surface properties of advanced materials are crucial for their activities regarding relevant applications, especially when chemical reactions occur on the surface. Electron-trap distribution analysis is usually performed by using a wide spectrum of techniques, including X-ray diffraction (XRD), X-ray photoelectron spectroscopy (XPS), UV−visible (vis) photoabsorption spectroscopy, Fourier transform infrared (FT-IR), Raman and photoluminescence (PL) spectroscopy, and surface area analysis according to Brunauer−Emmett−Teller (BET) theory. Nevertheless, the results obtained by those methods usually do not provide any remarkable differences between active and relatively inactive samples or are very difficult to correlate changes in surface properties with activity in specific applications. Thus, the results obtained by currently available techniques are usually not sufficient to draw conclusions about the mode of action of the material. Therefore, new, complementary methods, providing deeper analysis of the surface, are needed to elucidate the issue.

Among all materials, solid matters possessing photocatalytic properties attract our attention due to their possible employment in pollutant degradation, hydrogen generation, and carbon dioxide photoconversion using solar or low-powered light. It is known now that surface electronic properties determine the photoactivity and the mechanism of their photocatalytic performance; however, there is no quantitative method that allows for certainly the prediction of activity based on the measured electronic structure properties. In view of this, identifying those features may answer the main question about

the reason for the enhanced activity of the modified titania (TiO_2) photocatalysts under visible irradiation. Modification of titania is performed to activate them under vis irradiation from the viewpoint of practical applications and commercial benefits.[1] One of the effective methods is the application of ionic liquids (ILs) as structuring agents, which possess surface activity during titania synthesis.[2]

To date, the proposed mechanisms of the vis-light photoactivity enhancement of titania prepared in the presence of ILs were as follows: (i) doping of the titania lattice with non-metal elements derived from the IL structure;[2,3] (ii) favoring the formation of oxygen vacancies and the Ti^{3+} species (electron traps, ETs) by IL;[2,4] (iii) promoting titania hollow structure formation, thereby shortening the diffusion length of the charge carriers as well as increasing the number of reactive sites;[4] (vi) interaction of the bromide anion and molecular oxygen with the titania surface with formation of surface complex.[5]

To elucidate the surface electronic properties of the photocatalysts, Ohtani et al. developed a novel analytical method, namely, reversed double-beam photoacoustic spectroscopy (RDB-PAS).[6] This approach enables us to determine
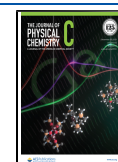
Table 1. Physical and Structural Properties of Samples Prepared with or without ILs Measured by Conventional Analytical Methods[2,11,12,a]

code[b]	specific surface area (m² g⁻¹)	pore volume (cm³ g⁻¹)	unit-cell parameters			crystallite size (nm)	surface content (%)[d]				phenol degradation under Vis (%)[e]
			a (nm)	c (nm)	volume (nm³)		Ti	Ti³⁺[c]	C	N	
no-IL	184	0.069	0.379	0.950	0.136	6.3	29.44	2.41	4.15	0.14	4
BPy (1:8)	214	0.104	0.377	0.951	0.135	5.3	—	—	—	—	18
EAN (1:8)	211	0.102	0.377	0.951	0.135	5.5	24.32	4.56	11.61	0.31	19
BPy (1:10)	213	0.104	0.377	0.949	0.135	5.8	—	—	—	—	22
EAN (1:10)	190	0.093	0.377	0.951	0.135	5.5	—	—	—	—	28
EAN (1:5)	216	0.105	0.377	0.951	0.135	6.5	—	—	—	—	33
BPy (1:1)	198	0.097	0.379	0.949	0.137	8.5	—	—	—	—	34
EAN (1:3)	216	0.105	0.379	0.953	0.137	6.0	—	—	—	—	36
BPy (1:5)	213	0.104	0.378	0.952	0.136	4.8	—	—	—	—	45
BPy (1:3)	215	0.105	0.377	0.951	0.136	4.9	26.80	6.66	10.55	0.07	58
TPTZ (1:10)	227	0.110	0.379	0.949	0.136	5.7	24.36	7.87	13.20	0.17	74
HDPyr (1:1)	188	0.092	0.378	0.950	0.136	5.4	23.51	6.58	14.90	0.15	79
EAN (1:1)	221	0.108	0.378	0.948	0.136	6.0	23.31	6.66	13.24	0.38	82
TBMA (1:2)	215	0.103	0.378	0.951	0.136	6.3	26.45	4.17	8.55	0.83	91

[a]Sorting was made with an increasing order of photocatalytic activity (phenol degradation). [b]no-IL: prepared without using IL. BPy, EAN, TPTZ, HDPyr, and TBMA show 1-butylpyridinium chloride ([BPy][Cl]), ethylammonium nitrate ([EAN][NO₃]), 2,3,5-triphenyltetrazolium chloride ([TPTZ][Cl]), hexadecylpyridinium chloride ([HDPyr][Cl]), and tributylmethylammonium chloride ([TBMA][Cl]), respectively. Ratios in parentheses show the molar ratio of IL and TBOT. [c]An XPS peak at 457 eV. [d]Dash means "not measured". [e]Degradation (decrease in concentration) of phenol by vis irradiation (>420 nm) under aerated conditions for 1 h.

the energy-resolved distribution of electron trap (ERDT) and conduction band bottom (CBB) positions reflecting a surface structure and a bulk structure, respectively, of the materials in the form of powder or thin films. In this method, direct photoexcitation of electrons from the valence band (VB) to empty (vacant) electronic levels (ETs) by wavelength-scanned continuous monochromatic light resulted in an accumulation of electrons in ETs (photoreaction) from the lower-energy side to the higher-energy side. Detection of the photoabsorption signal of the accumulated electrons in ETs by photoacoustic spectroscopy provided information on the amount (or density) of electron-filled ETs, and thus the total density of ETs. For a given pair of samples, the degree of coincidence (ζ) of ERDT/CBB patterns is determined, revealing the clear dependence between ζ and photoactivity: the higher is the ζ value, the higher is the degree of coincidence for the activity of the photocatalysts (ζ_{PC}). To date, this relation was confirmed for titania,[6] copper, cerium and/or platinum-modified titania,[7] and O, S-doped carbon nitride (C_3N_4).[8] Moreover, the doped atoms (unlike the precursors) were found to affect the ERDT/CBB patterns.[8] However, the surface electronic properties of the photocatalysts formed in the presence of ILs or other structure active agents were, to date, not analyzed. Structuring agent-assisted methods are very popular since they are effective in controlling the structure and morphology of the materials, which, in turn, favor the electronic transfer and enhance the optical absorption and photocatalytic performance.[9]

To date, research performed in the area of titania modification with ILs revealed a possible linkage between the mechanism of titania photoexcitation under vis light and the chemical structure of the ionic liquid used during preparation. Nevertheless, we still do not know how the IL's composition affects the surface properties of titania and thereby photoactivity. One of the premises is the relatively low thermal stability of IL under the preparation conditions (possible decomposition).[10] However, there are also ILs which are thermally stable and still reveal relatively high photoactivity.

In this regard, we characterized the surface and bulk electronic properties of the titania photocatalysts modified with the selected ionic liquids using the RDB-PAS technique to obtain ERDT patterns as a fingerprint of different ILs used for synthesis as well as IL-titania precursor (TBOT) molar ratio. For these experiments, the IL-titania samples with exceptionally high photoactivity determined by the model phenol degradation reaction under vis irradiation were selected. These are photocatalysts prepared by using ethylammonium nitrate [EAN][NO₃], 1-butylpyridinium chloride [BPy][Cl], hexadecylpyridinium chloride [HDPyr][Cl], tributylmethylammonium chloride [TBMA][Cl], and 2,3,5-triphenyltetrazolium chloride [TPTZ][Cl]. Four of these ILs undergo decomposition during solvothermal titania preparation to a large extent. In such a way, IL may become a source of elements incorporated in the titania structure. The fifth one, [HDPyr]-[Cl], is characterized by high photoactivity, but the efficiency of ILs decomposition during synthesis was much lower in comparison with above-mentioned ILs (more stable IL). For determining additional possible fingerprints, the samples prepared with various [EAN][NO₃]-TBOT and [BPy][Cl]-TBOT molar ratios, with much lower photoactivity, were also analyzed.

■ EXPERIMENTAL SECTION

Materials. Titanium(IV) butoxide (TBOT, 99%, Alfa Aesar, Germany), anhydrous ethyl alcohol (99.8%, POCh S.A. Poland), hydrochloric acid (36%, POCh S.A. Poland), and ionic liquids (ethylammonium nitrate, 1-butylpyridinium chloride, hexadecylpyridinium chloride, tributylmethylammonium chloride, and 2,3,5-triphenyltetrazolium chloride) (purveyed with at least ≥97% of purity, IOLITEC, Germany) have been applied during synthesis.

Preparations of IL-Assisted Titania Microspheres. The synthesis of the IL-TiO$_2$ particles was carried out according to the procedure described previously by our group.[2,5] Briefly, TBOT, used as a precursor of titania, was dispersed in absolute ethanol under constant vigorous stirring. In the next step, hydrochloric acid, distilled water, and appropriate IL were added. The amount of IL, calculated as the IL:TBOT molar ratio, was presented in Table 1. Afterward, the mixture was transferred into a Teflon-lined stainless-steel autoclave and incubated at 453 K for 24 h. Subsequently, the autoclave was cooled to room temperature and the resultant product was washed with ethanol and deionized water several times, dried overnight at 60 °C, and finally calcinated at 473 K for 2 h. For comparison, the pristine titania sample was synthesized using the same procedure except for IL addition.

Characterization by Conventional Techniques. The phase composition of the titania samples was estimated from power X-ray diffraction (XRD) measurements using a Rigaku MiniFlex 600 diffractometer equipped with copper Kα irradiation in the 2θ range of 20−80°. The average crystallite size was calculated using the Scherrer equation. The Brunauer−Emmett−Teller (BET) surface area and pore size of the photocatalysts was calculated by a Micromeritics Gemini V200 instrument (provided by Shimadzu) equipped with a VacPrep 061 Degasser. All samples were degassed at 473 K prior to the nitrogen adsorption measurements. The surface area was determined by using the multipoint BET method using the adsorption data in the relative pressure (P/P_0) range of 0.05−0.3. All data analysis were repeated and checked three times. The standard deviation of the BET surface areas was in the range of 1−4%. The physical and structural properties of a part of those titania samples have been reported previously.

Photocatalytic Activity Measurements. Photoactivity under vis irradiation was determined using phenol as a model compound, as we described previously.[2,11,12] The photocatalyst (0.125 g) was dispersed in 25 mL of phenol solution (0.21 mmol dm^{-3}) and poured into a cylindrical reactor with a quartz window. The suspension was aerated (5 dm^3 h^{-1}) and degradation experiments were performed at a temperature of 10 ± 0.5 °C, which was maintained via a water bath. As an irradiation source, a 1000 W xenon lamp (Model 6271H, Oriel) with an optical filter of >420 nm, GG 420 was used (the illumination intensity was equal to approximately 3 mW/cm^2). The phenol concentration was determined by the spectrophotometric method (λ_{max} = 480 nm) using a UV−vis spectrophotometer (Evolution 220, Thermo Scientific). The photocatalytic degradation runs were preceded by a blind test in the absence of photocatalysts or illumination. All data analysis was repeated and checked three times. The average standard deviation of the photoactivity measurements was below 1%.

Measurement of ERDT/CBB Patterns. In this study, a laboratory-made RDB-PAS instrument (code name BK1) was used. BK-1 is composed of a grating monochromator with a xenon lamp (Bunkokeiki M10-RP/BXL-150), a 625 nm LED (Luxeon LXHL-ND98) intensity modulated at 35 Hz by a digital function generator (NF Corporation DF-1906), a UV quartz combiner light guide (Moritex MXS5-1000S-UV3), a digital lock-in amplifier (NF Corporation LI5630) and a laboratory-made photoacoustic (PA) cell equipped with a quartz window, gastight bulbs, a MEMS (microelectromechanical system) microphone module (SparkFun MEMS Microphone Breakout, INMP401 (ADMP401)) and a stainless-steel sample holder.

Typical RDB-PAS measurement procedures are as follows.[6−8] Sample powder (ca. 50−100 mg) was loaded on a stainless sample holder and placed in a PA cell. The cell was transferred to a cubic acrylic box. Methanol-saturated nitrogen was introduced in the cell for at least 30 min to remove oxygen, and then the cell was sealed tightly. Two light beams were introduced to the cell through a quartz window. One is a continuous monochromatic light wavelength scanned from a longer wavelength to a shorter wavelength (typically 600−300 nm) with a 5 nm step. The other is an intensity-modulated (35 Hz) 625 nm LED light. The PA signal was amplified with a lock-in amplifier and recorded as RDB-PA spectrum showing the accumulation of electrons in ETs as shown in Figure 1. The spectrum was differentiated from the lower energy side to obtain an ERDT pattern followed by calibration with experimentally determined conversion coefficient[6] to the absolute density of ETs. The energy of ETs is shown regarding the valence band top (VBT) energy for convenience and thus the obtained ERDT pattern was replotted as a bar graph with a pitch of 0.05 eV as shown in, e.g., Figure 2.

The conduction-band bottom (CBB) energy was estimated by (single beam) PAS using the same setup. The sample in a PA cell was irradiated by a modulated (80 Hz) monochromatic light wavelength scanned from a longer wavelength to a shorter wavelength to obtain the PA spectrum, which was then calibrated with a spectrum of carbon black. To determine the absorption edge wavelength, the bandgap energy in the unit of eV was calculated and plotted as CBB regarding VBT as shown in, e.g., Figure 1.

■ RESULTS AND DISCUSSION

Physical and Structural Properties Measured by Conventional Analytical Methods. To identify the surface and bulk electronic properties of IL-modified titania, the samples with particularly high photocatalytic performance, as determined by the model phenol degradation reaction under vis irradiation, were selected and synthesized by the solvothermal method. These photocatalysts were prepared with addition of ethylammonium nitrate (EAN_TiO$_2$), 1-butylpyridinium chloride (BPy_TiO$_2$), tributylmethylammonium chloride (TBMA_TiO$_2$), 2,3,5-triphenyltetrazolium chloride (TPTZ_TiO$_2$), or hexadecylpyridinium chloride (HDPyr_TiO$_2$). Precise characteristics of the EAN_TiO$_2$, BPy_TiO$_2$, and TPTZ_TiO$_2$ samples were previously published.[2,10−12] Nevertheless, the most crucial elements needed for the analysis and discussion presented in this manuscript were repeated below. Basic description of the samples and their photocatalytic activity determined under vis irradiation (the range of 51−91% of phenol degradation) is shown in Table 1.[10]

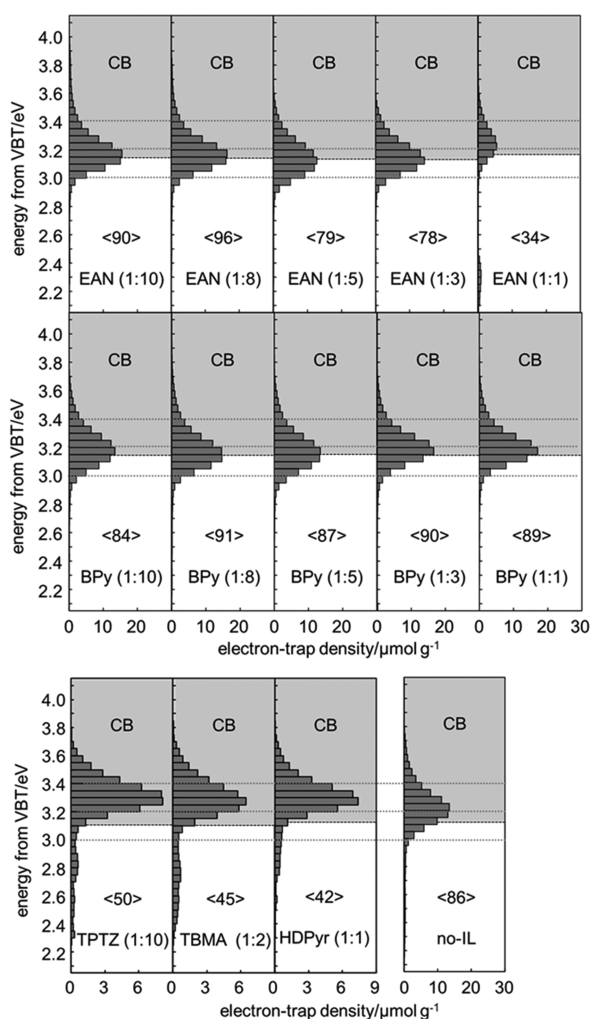Different levels of thermal decomposition of the selected ionic liquids were detected during solvothermal treatment

Figure 1. ERDT/CBB patterns of IL-TiO$_2$ samples and no-IL. The bottom dashed line of each gray box (conduction band) represents CBB conduction band bottom. Figures in < > show the total density of electron traps in the unit of μmol g^{-1}. Three gray dotted lines correspond to the energy of the valence band top of 3.4, 3.2, and 3.0 eV.
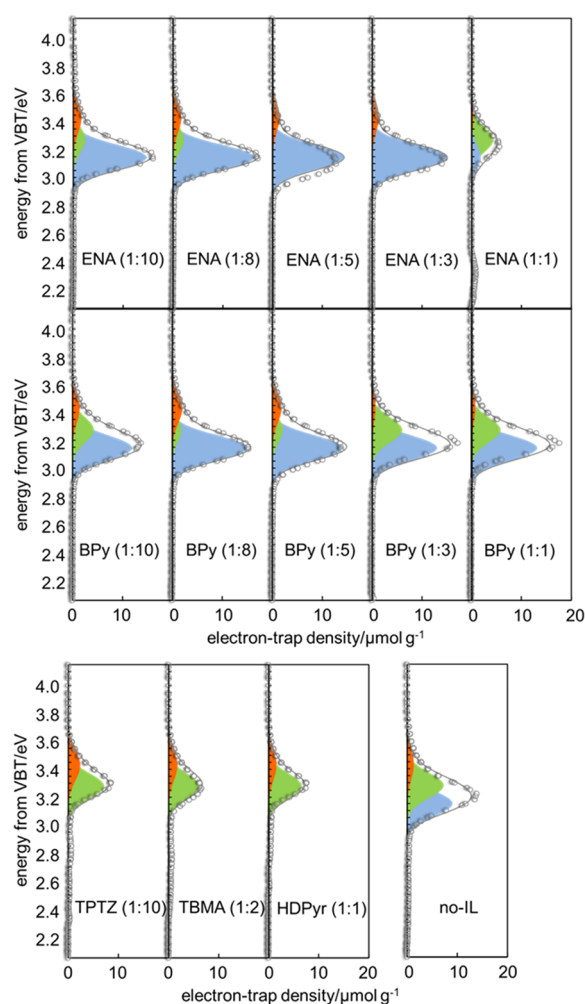

Figure 2. Deconvoluted ERDT/CBB patterns of IL-TiO$_2$ samples and no-IL. Blue, green, and red peaks correspond to 3.15, 3.28, and 3.43 eV peaks with peak widths (fwhm) of 0.09, 0.09, and 0.11 eV, respectively. Circles and solid lines are the actual measured data and the summation of deconvoluted peaks, respectively.

performed at 473 K. The most susceptible ones to thermal decomposition in the chosen conditions were three of them, namely, [TPTZ][Cl], 100%, [EAN][NO$_3$], 97%, [TBMA]-[Cl], 95%. The fourth one, [BPy][Cl], decomposed by 50%, whereas the last one, [HDPyr][Cl], was the most stable (12% of decomposition).[10] Additionally, samples with various concentrations of IL ([EAN][NO$_3$] and [BPy][Cl]) in the reaction environment, represented as the IL:TBOT molar ratio, were also prepared (Table 1). These samples revealed much lower photoactivity, also shown in Table 1.

All IL_TiO$_2$ photocatalysts revealed developed surface area in comparison with pristine titania used as a reference sample. This parameter increased from 184 m^2 g^{-1} detected for the reference titania (no-IL) to 215−227 m^2 g^{-1} determined for TiO$_2$ prepared in a presence of [EAN][NO$_3$], [BPy][Cl], [TBMA][Cl], and [TPTZ][Cl], except for a few samples of EAN_TiO$_2$ (1:10), BPy_TiO$_2$ (1:1), and HDPyr_TiO$_2$ (1:1) with their specific surface area ranging 188−198 m^2 g^{-1}. The pore size of IL-modified samples was approximately 0.1 cm^3 g^{-1}, being a little larger than that of no-IL (0.065 cm^3 g^{-1}). Nevertheless, these results suggested that the use of ILs in the

preparation process tended to give slightly higher specific surface area and larger pore size, although such properties seem not to be directly related to their photocatalytic activity.

The XRD analyses confirmed that anatase was solely formed (no other crystalline phase was found), although this does not exclude the possible presence of XRD-inert amorphous phase in the samples. All diffraction peaks were well indexed to the tetragonal structure (space group number 141, $I41/amd$). The size of the crystallites was estimated from the Scherrer formula, based on the 101-peak width (25.3°). Reflecting the observed relatively broad XRD peaks, a small size of crystallite in the range of 4.8−8.5 nm was estimated. Unit-cell parameters, length of a ($a = b$) and c and volume, were almost constant, suggesting a negligible influence on the crystalline structure of the preparation in the presence of IL and those crystalline structural properties seem not to account for the difference in photocatalytic activities.

The contents of titanium, carbon, and nitrogen in the part of the samples were listed in Table 1. The appreciable contents of carbon and nitrogen in no-IL were attributable to the remaining organic residues of a source titanium alkoxide and unknown contamination, respectively. Compared with those contents in the no-IL sample, the titania samples prepared in

Table 2. Parameters of ERDT/CBB Patterns of Samples[a]

				deconvolution			
code[b]	CBB (eV)	peak energy (eV)	total ET density (μmol g^{-1})	total density	$d_{3.15}$:$d_{3.28}$:$d_{3.43}$	$d_{3.28}$ (+ $d_{3.43}$) (%)	phenol degradation under Vis (%)[c]
no-IL	3.10	3.175	86	82	41:33:08	40 (50)	4
BPy (1:8)	3.15	3.125	91	87	68:08:11	9 (22)	18
EAN (1:8)	3.15	3.125	96	93	74:10:09	10 (20)	19
BPy (1:10)	3.15	3.175	84	81	54:19:08	23 (33)	22
EAN (1:10)	3.15	3.175	90	87	67:11:09	12 (23)	28
EAN (1:5)	3.15	3.125	79	73	65:00:08	0 (11)	33
BPy (1:1)	3.15	3.175	89	91	60:26:05	30 (34)	34
EAN (1:3)	3.15	3.125	78	75	68:00:07	0 (9)	36
BPy (1:5)	3.15	3.175	87	83	63:09:11	11 (24)	45
BPy (1:3)	3.15	3.175	90	90	59:27:04	30 (34)	58
TPTZ (1:10)	3.10	3.275	50	45	00:32:13	71 (100)	74
HDPyr (1:1)	3.10	3.275	42	40	00:30:10	75 (100)	79
EAN (1:1)	3.15	3.225	34	30	08:20:02	67 (73)	82
TBMA (1:2)	3.10	3.275	45	37	00:27:10	73 (100)	91

[a]Sorting was made with an increasing order of photocatalytic activity (phenol degradation). [b]no-IL: prepared without using IL. BPy, EAN, TPTZ, HDPyr, and TBMA show 1-butylpyridinium chloride ([BPy][Cl]), ethylammonium nitrate ([EAN][NO$_3$]), 2,3,5-triphenyltetrazolium chloride ([TPTZ][Cl]), hexadecylpyridinium chloride ([HDPyr][Cl]), and tributylmethylammonium chloride ([TBMA][Cl]), respectively. Ratios in parentheses show the molar ratio of IL and TBOT. [c]Degradation (decrease in concentration) of phenol by vis irradiation (>420 nm) under aerated conditions for 1 h.

the presence of ILs has appreciably low titanium content and high carbon and nitrogen contents, indicating the existence of remaining IL or its decomposed products. It seems no clear correlation of carbon and nitrogen contents with the photocatalytic activity as less active EAN (1:8) showed high carbon and nitrogen contents, but these remaining organic residues for ILs will be discussed later.

The XPS measurements suggested the presence of trivalent titanium species (Ti^{3+}; ca. 457 eV) in titania particles in the amount differing with the type of ILs chosen for preparation (Table 1). Since even no-IL possessed Ti^{3+}, Ti^{3+} might be created during sample preparation and/or evacuation in the XPS chamber caused by the remaining organic residues from TBOT and/or ILs. The slightly yellow color, due to photoabsorption of blue light for a part of the samples also suggested the Ti^{3+} formation. According to experimental results and theoretical calculations, the Ti^{3+} centers could create donor levels in the electronic structure of TiO$_2$, and the excess electrons affect the surface adsorption and reactivity of key adsorbates such as O$_2$ or H$_2$O on TiO$_2$.[13,14] However, the amount of Ti^{3+} species at ca. 457 eV in XP spectra seemed not to account for the difference in the photocatalytic activities (Table 1).

Thus, the structural and physical properties of the present samples measured by the conventional analytical techniques could not interpret the difference in their photocatalytic activity. It is worth noting that the conclusions were drawn from a study involving only one photocatalytic test considering one model pollutant (phenol). Nevertheless, the response of the photocatalyst may vary for contaminants with different structures, which may be due to differences in the affinity of the contaminant for the photocatalyst surface.[13,15] In this regard, to achieve a deeper understanding of the properties of titania obtained in the presence of ILs, it is worthwhile to use a wider range of model impurities with different structures, which will be the subject of further research.

Structural Properties Measured by RDB-PAS. Figure 1 shows the ERDT/CBB patterns of the samples used in this study.

The energy of CBB, position and shape of a peak (peaks), and total density of electron traps seemed similar to the ordinary commercial anatase titania particles,[6,16] but some samples showed a little different ERDT-pattern position and shape, i.e., peak position of EAN (1:1), TPTZ (1:10), HDPyr (1:1), and TBMA (1:2) were a little shifted to the higher-energy side compared with those of the others. Table 2 summarizes the parameters of ERDT/CBB patterns of the samples as well as their photocatalytic activity (same as those in Table 1).

Conduction-band bottom (CBB) position (energy), corresponding to the bandgap energy, was all in the range of 3.10−3.15, similar to the commercial anatase powders reflecting the bulk crystalline structure, anatase, of the samples. The total ET density of the samples was also not different from each other except for the reference sample no-IL. It has been reported that ETs in, at least, titania samples are predominantly located on the surface and thereby the total ET density is increased roughly in proportion to the specific surface area.[6] Therefore, the total ET density might reflect the similarity/slightly differentness of the specific surface area of samples. However, it is noticeable that the higher photocatalytic activity samples (>70% phenol degradation) contained appreciably low total density, although their specific surface areas were almost the same as those other samples, presumably due to the relatively low density of amorphous phases as discussed below.

On the other hand, the peak position (energy) of ERDT patterns showed the clear tendency that the higher the peak energy was, the higher the photocatalytic activity was observed. Taking into account that ETs measured in RDB-PAS are predominantly located on the sample surface, it is suggested that the surface of the samples was modified to improve the photocatalytic activity in the solvothermal process in the presence of ILs, from the original anatase surface without the

change in bulk structure. Then, what does the higher energy shift mean?

Recently, it has been reported that the braying (grinding)-induced surface amorphization of rutile[17] and anatase/brookite powders was detected by RDB-PAS;[17] the ERDT peak of nonbrayed sample was slightly shifted by grinding, attributable to the amorphization of crystallite surface and further braying (grinding)-induced the appearance of a high-energy (ca. 3.4 eV) amorphous peak. Since the high-energy and slightly shifted peaks were observed for a commercial amorphous sample alone and its mixture with crystalline titania, respectively, they were attributed to an isolated amorphous phase and amorphous layer in contact with the crystalline surface.[17] Such a shift of the amorphous peak by contacting with crystalline titania is accounted for the interparticle charge-transfer excitation (ICTE).[16] On the basis of these considerations, the slight high-energy shift of the IL-TiO$_2$ samples is attributable to the formation of the surface amorphous layer. Their asymmetrical peaks with longer tailings in the high-energy side seem consistent with the presumed surface amorphization, since the amorphous peaks tend to have a larger width compared with those of crystallites.[17]

Then, peak deconvolution was performed by assuming that the actual peak is composed of anatase and two kinds of amorphous peaks of Gaussian-function curves with appropriate peak positions and peak width (full width at half maxima = fwhm). Reasonable results (Figure 2) were obtained by assuming three peaks of position, 3.15, 3.28, and 3.43 eV, and fwhm, 0.09, 0.09, and 0.11 eV, respectively, with the exception of a less reproduced pattern of EAN (1:5). Based on the reported discussion, these three peaks are assigned to electron traps on the surface of anatase, an amorphous phase in contact with anatase, and an isolated amorphous phase, respectively. Compared with the photocatalytic activity for phenol degradation, it was obvious that the titania samples showing higher photocatalytic activity, >70% phenol degradation, contained higher content, $d_{3.28}$ > 70%, of those amorphous phases. The relatively low total electron-trap density of those samples might be explained by the low surface density of electron traps of the amorphous phase compared to anatase.

It has been reported that amorphous titania without any crystalline phase showed negligible photocatalytic activity in a few reactions systems,[18] and amorphization of a rutile titania photocatalyst induced the deactivation. As far as the authors know, there have been published no papers reporting appreciable photocatalytic activity of the amorphous phase of metal-oxide photocatalysts and/or enhancement of photocatalytic activities by amorphous phases. Therefore, it is reasonable to assume that the amorphous phases themselves do not enhance the activity of IL-TiO$_2$ samples, but the formation of those amorphous phases is related to the modification of the surface structure(s) during the fabrication process in the presence of ionic liquids to enhance the activity. This is consistent with the fact that the no-IL sample, containing rather high amounts of amorphous phase (>40%), showed negligible activity.

One of the possible explanations is the surface coverage by ionic liquids or organic hydrophobic residues as a decomposition product of ionic liquids to promote surface amorphization and termination of the amorphous surface with organic residues; the adsorption of the substrate, phenol, may be enhanced by the hydrophobic surface. It seems

reasonable to find such amorphization for the samples prepared in the presence of relatively more hydrophobic cation ILs such as TPTZ, TBMA, or HDPyr and in the presence of large amounts of IL such as EAN (1:1) and their relatively low total electron-trap density as describe in the preceding section. For the enhance phenol adsorption, however, blank experiments on phenol adsorption on the surface showed that the change in concentration of phenol by suspending titania samples was too small to determine and thereby it was impossible to confirm the enhanced phenol adsorption with sufficient accuracy.

Figure 3 shows ERDT patterns of the EAN (1:1) sample before and after ozone treatment; ozone-containing oxygen
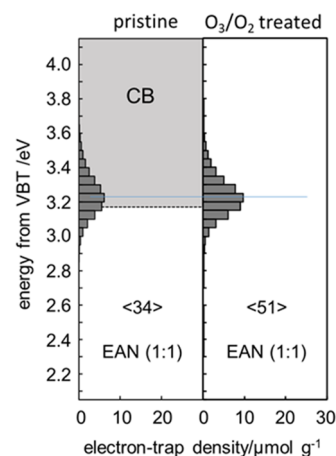

Figure 3. ERDT/CBB patterns of EAN (1:1) before and after room-temperature ozone treatment. Figures in < > show the total density of electron traps in the unit of μmol g^{-1}.

was made to flow through the PAS cell under ambient temperature before the RDB-PAS measurement. The ozone treatment clearly increased the total electron-trap density, negligibly changing the ERDT-pattern shape; the degree of coincidence of ERDT patterns (ζS)[6] before and after ozone treatment was >0.90, suggesting almost the same shape. This result can be reasonably interpreted on the assumption that the possible organic residues capping electron traps on the surface of amorphous phases were removed, at least partly, by undergoing oxidative degradation by ozone.

◼ CONCLUSIONS

On the basis of the studies on energy-resolved distribution of electron traps on titania samples prepared in the presence (and absence) of ILs, it was revealed that a group of samples exhibiting relatively high photocatalytic activity of phenol degradation contained surface amorphous layers, giving higher energy side peaks in their ERDT patterns, while a group of samples of the low activity had negligible such amorphous layers. This information could not be obtained by the results of conventional structural analyses such as XRD and XPS. Considering the reported negligible photocatalytic activity of amorphous titania, the reason for the high photocatalytic activities of the samples can be assigned to ILs or organic residues originated from ILs giving surface hydrophobicity to enhance the adsorption of the reaction substrate, phenol, on the photocatalyst surface. The XPS analysis also gave results on the amount of organic residues, although the carbon and/or nitrogen surface contents were not directly related to the

photocatalytic activity. The possible explanation is that the organic residues induce two types of surface structure; one is the amorphous surface layer covered with hydrophobic organic residues and the others is the (crystalline) surface covered with hydrophilic, probably ionic, organic residues, and both residues were equally detected in the XPS analysis.

Thus, ERDT/CBB patterns of samples measured by RDB-PAS provide structural information closely related to the actual photocatalytic activity, which cannot be suggested using only the conventional structural analyses methods.

■ AUTHOR INFORMATION

Corresponding Authors

Adriana Zaleska-Medynska − *Department of Environmental Technology, Faculty of Chemistry, University of Gdansk, 80-308 Gdansk, Poland;* ⊙ orcid.org/0000-0003-3817-296X; Email: adriana.zaleska-medynska@ug.edu.pl

Bunsho Ohtani − *Institute for Catalysis, Hokkaido University, Sapporo 001-0021, Japan*; Email: ohtani@cat.hokudai.ac.jp

Authors

Justyna Łuczak − *Department of Process Engineering and Chemical Technology, Faculty of Chemistry, Gdańsk University of Technology, 80-233 Gdansk, Poland;* ⊙ orcid.org/0000-0001-9939-7156

Anna Pancielejko − *Department of Process Engineering and Chemical Technology, Faculty of Chemistry, Gdańsk University of Technology, 80-233 Gdansk, Poland*

Guangyi Chen − *Institute for Catalysis, Hokkaido University, Sapporo 001-0021, Japan*

Mai Takashima − *Institute for Catalysis, Hokkaido University, Sapporo 001-0021, Japan;* ⊙ orcid.org/0000-0001-6416-3704

Complete contact information is available at:
https://pubs.acs.org/10.1021/acs.jpcc.1c09174

Author Contributions

The manuscript was written through contributions of all authors. All authors have given approval to the final version of the manuscript.

Notes

The authors declare no competing financial interest.

■ REFERENCES

(1) Schneider, J.; Matsuoka, M.; Takeuchi, M.; Zhang, J.; Horiuchi, Y.; Anpo, M.; Bahnemann, D. W. Understanding TiO2 Photocatalysis: Mechanisms and Materials. *Chem. Rev.* **2014**, *114* (19), 9919−9986.

(2) Paszkiewicz-Gawron, M.; Długokęcka, M.; Lisowski, W.; Paganini, M. C.; Giamello, E.; Klimczuk, T.; Paszkiewicz, M.; Grabowska, E.; Zaleska-Medynska, A.; Luczak, J. Dependence between Ionic Liquid Structure and Mechanism of Visible-Light-Induced Activity of TiO2 Obtained by Ionic-Liquid-Assisted Solvothermal Synthesis. *ACS Sustainable Chem. Eng.* **2018**, *6* (3), 3927−3937.

(3) Li, F.; Wang, X.; Zhao, Y.; Liu, J.; Hao, Y.; Liu, R.; Zhao, D. Ionic-Liquid-Assisted Synthesis of High-Visible-Light-Activated N-B-F-Tri-Doped Mesoporous TiO2 via a Microwave Route. *Appl. Catal., B* **2014**, *144*, 442−453.

(4) Chen, Y.; Li, W.; Wang, J.; Gan, Y.; Liu, L.; Ju, M. Microwave-Assisted Ionic Liquid Synthesis of Ti3+ Self-Doped TiO2 Hollow Nanocrystals with Enhanced Visible-Light Photoactivity. *Appl. Catal., B* **2016**, *191*, 94−105.

(5) Łuczak, J.; Paszkiewicz-Gawron, M.; Długokęcka, M.; Lisowski, W.; Grabowska, E.; Makurat, S.; Rak, J.; Zaleska-Medynska, A. Visible-Light Photocatalytic Activity of Ionic Liquid TiO2 Spheres: Effect of the Ionic Liquid's Anion Structure. *ChemCatChem* **2017**, *9* (23), 4377−4388.

(6) Nitta, A.; Takase, M.; Takashima, M.; Murakami, N.; Ohtani, B. A Fingerprint of Metal-Oxide Powders: Energy-Resolved Distribution of Electron Traps. *Chem. Commun.* **2016**, *52* (81), 12096−12099.

(7) Unwiset, P.; Chen, G.; Ohtani, B.; Chanapattharapol, K. C. Correlation of the Photocatalytic Activities of Cu, Ce and/or Pt-Modified Titania Particles with Their Bulk and Surface Structures Studied by Reversed Double-Beam Photoacoustic Spectroscopy. *Catalysts* **2019**, *9* (12), 1010.

(8) Chuaicham, C.; Karthikeyan, S.; Pawar, R. R.; Xiong, Y.; Dabo, I.; Ohtani, B.; Kim, Y.; Song, J. T.; Ishihara, T.; Sasaki, K. Energy-Resolved Distribution of Electron Traps for O/S-Doped Carbon Nitrides by Reversed Double-Beam Photoacoustic Spectroscopy and the Photocatalytic Reduction of Cr(Vi). *Chem. Commun.* **2020**, *56* (26), 3793−3796.

(9) Liang, Q.; Liu, X.; Zeng, G.; Liu, Z.; Tang, L.; Shao, B.; Zeng, Z.; Zhang, W.; Liu, Y.; Cheng, M.; et al. Surfactant-Assisted Synthesis of Photocatalysts: Mechanism, Synthesis, Recent Advances and Environmental Application. *Chem. Eng. J.* **2019**, *372* (February), 429−451.

(10) Rybińska-Fryca, A.; Mikolajczyk, A.; Łuczak, J.; Paszkiewicz-Gawron, M.; Paszkiewicz, M.; Zaleska-Medynska, A.; Puzyn, T. How Thermal Stability of Ionic Liquids Leads to More Efficient TiO2-Based Nanophotocatalysts: Theoretical and Experimental Studies. *J. Colloid Interface Sci.* **2020**, *572*, 396−407.

(11) Paszkiewicz-Gawron, M.; Gołąbiewska, A.; Pancielejko, A.; Lisowski, W.; Zwara, J.; Paszkiewicz, M.; Zaleska-Medynska, A.; Łuczak, J. Impact of Tetrazolium Ionic Liquid Thermal Decomposition in Solvothermal Reaction on the Remarkable Photocatalytic Properties of TiO2 Particles. *Nanomaterials* **2019**, *9* (5), 744.

(12) Gołąbiewska, A.; Checa-Suárez, M.; Paszkiewicz-Gawron, M.; Lisowski, W.; Raczuk, E.; Klimczuk, T.; Polkowska, Ż.; Grabowska, E.; Zaleska-Medynska, A.; Łuczak, J. Highly Active TiO2Microspheres Formation in the Presence of Ethylammonium Nitrate Ionic Liquid. *Catalysts* **2018**, *8* (7), 279.

(13) Enríquez, R.; Agrios, A. G.; Pichat, P. Probing Multiple Effects of TiO2 Sintering Temperature on Photocatalytic Activity in Water by Use of a Series of Organic Pollutant Molecules. *Catal. Today* **2007**, *120* (2), 196−202.

(14) Thompson, T. L.; Yates, J. T. TiO2-Based Photocatalysis: Surface Defects, Oxygen and Charge Transfer. *Top. Catal.* **2005**, *35* (3−4), 197−210.

(15) Ohtani, B.; Mahaney, O. O. P.; Amano, F.; Murakami, N.; Abe, R. What Are Titania Photocatalysts?-An Exploratory Correlation of Photocatalytic Activity with Structural and Physical Properties. *J. Adv. Oxid. Technol.* **2010**, *13* (3), 247−261.

(16) Shen, Y.; Nitta, A.; Takashima, M.; Ohtani, B. Do Particles Interact Electronically?-Proof of Interparticle Charge-Transfer Excitation between Adjoined Anatase and Rutile Particles. *Chem. Lett.* **2021**, *50* (1), 80−83.

(17) Chen, G.; Takashima, M.; Ohtani, B. Direct Amorphous-Structure Analysis: How Are Surface/Bulk Structure and Activity of Titania Photocatalyst Particles Changed by Milling? *Chem. Lett.* **2021**, *50* (4), 644−648.

(18) Ohtani, B.; Ogawa, Y.; Nishimoto, S. I. Photocatalytic Activity of Amorphous-Anatase Mixture of Titanium(IV) Oxide Particles Suspended in Aqueous Solutions. *J. Phys. Chem. B* **1997**, *101* (19), 3746−3752.